RSC Advances

PAPER

View Article Online
View Journal | View Issue

Cite this: *RSC Adv.*, 2025, **15**, 36823

MOF modified with a Cu-complex as a novel MOF-based heterogeneous catalyst for the one-pot one-step synthesis of α-aminophosphonates directly from alcohols by a tandem oxidation process

Sara Sobhani,*[a] Alireza Paseban,[b] Roya Jahanshahi [c] and José Miguel Sansano [d]

A metal–organic framework functionalized with a copper complex, named Cu-ISA-MIL-Fe, was fabricated through post-synthetic modification of Fe-MIL-101-NH_2 *via* isatin Schiff-base formation followed by coordination with $Cu(OAc)_2$. The newly synthesized Cu-ISA-MIL-Fe was characterized by analytical methods, including PXRD, FT-IR, XPS, FESEM, EDS elemental mapping, TEM, and elemental analysis. The similarity of its PXRD pattern with that of Fe-MIL-101-NH_2 indicated that the crystalline structure of the MOF in the post-synthetic modification remained intact. FT-IR analysis endorsed the successful construction and functionalization of the MOF. FESEM and TEM images showed that the octahedral morphology of the MOF with an edge length of ~500 nm was well preserved. XPS elemental survey and EDS elemental mapping confirmed the existence of C, N, O, Cu and Fe, with a uniform distribution throughout the MOF structure. Cu-ISA-MIL-Fe was used as the first MOF-based catalyst for the one-pot one-step synthesis of dialkyl α-aminophosphonates directly from readily available alcohols *via* a tandem oxidation process. The catalyst showed an extremely high catalytic performance for the selective oxidation of different benzyl alcohols, followed by the condensation of the *in situ*-prepared benzaldehyde with anilines and alkyl phosphites (tri-ethyl/methyl/*iso*-propyl and di-*iso*-propyl phosphites) to produce a variety of dialkyl α-aminophosphonates. This methodology offers a number of merits, including cost-effective operational conditions, efficient and selective product formation in 75–95% yields, reduced reaction times, use of a green solvent, and facile catalyst separation and recyclability. Besides, conducting a simplified one-pot one-step synthetic procedure contributes to step saving, minimizes the procedural complexity and decreases waste production, further enhancing the overall efficiency of the method.

Received 25th August 2025
Accepted 17th September 2025

DOI: 10.1039/d5ra06341h

rsc.li/rsc-advances

1. Introduction

Nowadays, scientific research has advanced in addressing the significant challenges of green chemistry. In designing organic synthetic approaches, methodological efficiency and environmental compatibility are two fundamental principles that must be considered.[1,2] One of the most promising strategies in this regard is the simultaneous conduction of multiple reactions in a single reaction vessel without the need to separate the products at each stage through tandem transformations.[3,4] Applying this method not only minimizes the use of toxic solvents and reagents but also reduces waste, cost and time while increasing the overall safety.[4] Therefore, tandem reactions are highly attractive from both economic and environmental points of view.[3,4]

Carbonyl moieties serve as versatile synthetic building blocks for the fabrication of numerous bioactive and complex molecules that are commonly found in natural products.[5] They also play a crucial role in facilitating various substantial transformations between functional groups across diverse synthetic pathways.[6] The common strategy for the synthesis of aldehydes and ketones involves the oxidative transformations of primary and secondary alcohols, respectively, which are broadly accessible, inexpensive and easy to store and handle.[7] This approach has found widespread implementation across both industrial applications and academic research. In response to the important challenges in green chemistry, expanding the methods for alcohol oxidation to generate aldehydes, which subsequently undergo reactions with suitable reagents to generate C–C/C–N or C–P bonds, is known as a tandem oxidation process (TOP) and is highly desirable.[8]

[a]*Department of Chemistry, College of Science, Shiraz University, Shiraz, Iran. E-mail: sarasobhani@saadi.shirazu.ac.ir; Tel: +987136137198*
[b]*Department of Chemistry, College of Sciences, University of Birjand, Birjand, Iran*
[c]*Department of Chemical Engineering, Birjand University of Technology, Birjand, Iran*
[d]*Departamento de Química Orgánica, Centro de Innovación en Química Avanzada (ORFEO-CINQA) and Instituto de Síntesis Orgánica, Universidad de Alicante, Apdo. 99, 03080 Alicante, Spain*

α-Aminophosphonates represent a significant class of organophosphorus compounds owing to their structural resemblance to α-amino acids. They are important compounds due to their diverse applications in biochemistry,[9,10] medicinal chemistry,[11–14] life sciences,[11–14] and agriculture and industrial chemistry.[15–17] They demonstrate important bioactive features, comprising antibacterial, enzyme inhibition, anticancer and antifungal activities. Further, they can serve as pesticides, fungicides, insecticides, and plant growth regulators (Scheme 1).[18–21]

The most widely used synthetic procedure for α-aminophosphonates is the Kabachnik–Fields method.[22–25] This transformation involves a three-component condensation reaction of amine compounds, carbonyl-containing substrates, and phosphite esters.[22–25] This reaction proceeds *via* the hydrophosphorylation of an *in situ* formed Schiff-base, catalyzed by either acidic or basic catalysts.[26] Nevertheless, in the majority of reported protocols, the reactions were started from aldehydes as carbonyl compounds and mainly focused on utilizing various catalysts to enhance the reaction efficiency.[23–34] Employing alcohol derivatives as starting materials in the TOP-based synthesis of α-aminophosphonates widens the application scope of the Kabachnik–Fields method by means of using safer substrates aligned with green chemistry principles. To the best of our knowledge, only a limited number of synthetic protocols have been reported for the synthesis of these valuable scaffolds through the TOP strategy.[35–39] Despite their individual merits, these methods often suffer from significant shortcomings, including prolonged reaction times;[35,36,38] low product yields;[36,38] homogeneous and non-recyclable catalytic systems;[35,38] the use of structurally complex,[35] expensive,[35,39] or even explosive catalysts;[37] harsh reaction conditions;[35–39] and use of toxic solvents.[35,36,38,39] Most notably, the majority of these protocols involve one-pot two-step procedures,[35–38] which not only increases the operational complexity, energy, time and material consumption, but also reduces the overall synthetic efficiency. Among the reported studies, only one method has been described as a one-pot one-step approach.[39] However, even this method has been hindered by critical limitations, such as the use of costly catalysts and toxic solvents. These limitations highlight the crucial need for the development of more efficient, practical, and environmentally benign catalytic systems that can facilitate the one-pot one-step synthesis of α-aminophosphonates directly from alcohols *via* the TOP strategy.

Metal–organic frameworks (MOFs), composed of organic ligands and metal ions or clusters, have been widely used in numerous fields, including adsorption, separation, sensing, and catalysis.[40] Post-synthetic modification (PSM) has emerged as a promising strategy for the development of MOF-based heterogeneous catalysts *via* the incorporation of diverse functional moieties within their porous structures.[41] PSM techniques are particularly attractive for the synthesis of MOFs due to several distinct advantages.[42] First, the solvothermal reaction conditions typically utilized in MOF synthesis impose considerable constraints on the range of functional groups that can be incorporated during the pre-synthetic stage.[43] Second, the presence of organic ligand components within MOF structures (in contrast with many other crystalline inorganic solids) facilitates the application of diverse organic reactions, as established by synthetic organic chemists.[44] Ultimately, the intrinsic high porosity of MOF structures allows reagents to access the interior of their framework, enabling chemical functionalization not only on the external surface but also within the internal cavities of the MOFs.[45,46] Among MOFs, MIL-101-NH_2 is distinguished by its properties, including a rigid structure, high surface area, high porosity, and superb chemical and hydrothermal stability.[47] Moreover, the presence of amine groups in this type of MOF allows for PSM, enabling the preparation of a range of new MOF-based materials as efficient catalysts.[48]

Copper-based MOFs were mainly recognized for their application as Lewis acid catalysts. They can also be used in redox catalyses.[49] Due to the dual characteristics of copper, TOPs, in which the copper is able to act as a catalyst both in the oxidation step and in the subsequent reaction, can be

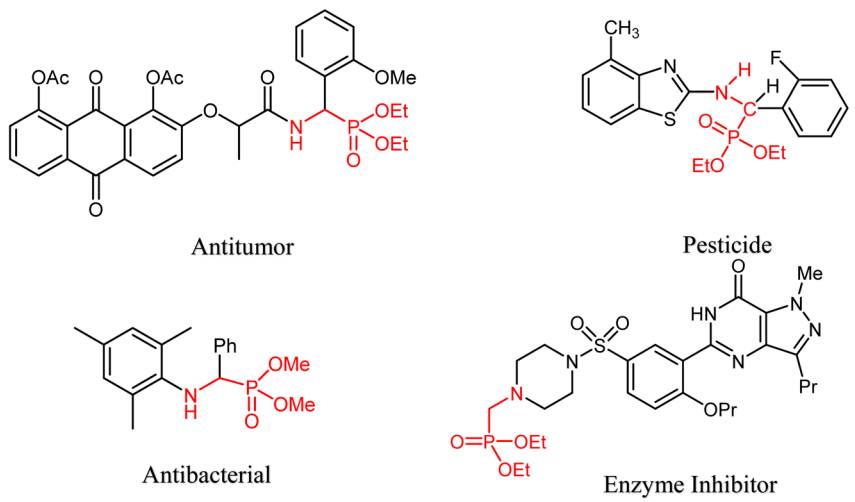

Scheme 1 Structures of some α-aminophosphonates with their biological activity.

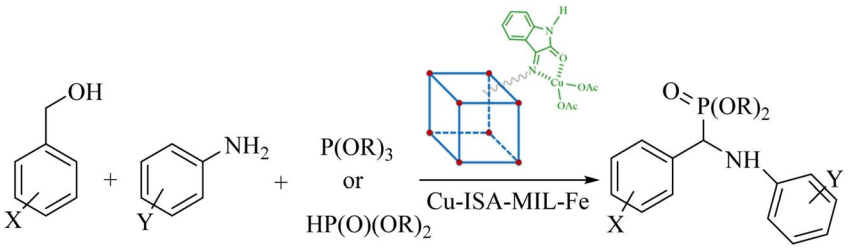

Scheme 2 One-pot one-step synthesis of α-aminophosphonates from alcohols *via* the TOP strategy, catalyzed by Cu-ISA-MIL-Fe.

performed in the presence of copper-based MOFs. In this regard, some TOPs, such as tandem alcohol oxidation-imine formation, deacetalization–Knoevenagel condensation reaction, epoxidation of olefin-cyclic carbonates synthesis, alcohol oxidation-Knoevenagel condensation, catalyzed by different types of copper-based MOFs, have been reported.[49,50] However, in spite of the high efficiency of copper-based MOFs, the reports on their application as catalysts in the TOP reactions are limited. Therefore, there is a lot of room for research in this area with new innovations.

As part of our continued efforts to establish novel tandem synthetic methods,[51] we have synthesized a new copper-based MOF denoted as Cu-ISA-MIL-Fe, through the PSM of Fe-MIL-101-NH_2, as the first MOF-based heterogeneous catalyst, which enables the direct one-pot one-step synthesis of α-aminophosphonates from alcohols *via* the TOP strategy (Scheme 2).

2. Experimental

2.1. Instrumentals

Crystallographic data were recorded on a PANalytical X'Pert Pro diffractometer equipped with Cu Ka radiation (λ = 1.540 Å). Infrared spectra were recorded on a Shimadzu FT-IR-8300 spectrometer. NMR spectra were recorded on a Bruker Advance DPX-300 using deuterated $CDCl_3$ as the solvent. Morphological and structural analyses were performed on a Philips CM30 transmission electron microscope (TEM) and a Mira 3-XMU field-emission scanning electron microscope (FESEM). The surface elemental composition and chemical states were studied by X-ray photoelectron spectroscopy (XPS) employing a VG-Microtech Multilab 3000 system equipped with an aluminum anode. The XPS spectral deconvolutions were accomplished *via* Gaussian–Lorentzian curve fitting. The elemental distribution and composition were further investigated by energy-dispersive X-ray spectroscopy (EDS) and elemental mapping analysis using a Tescan Mira3 microscope. The quantitative analysis of the copper content of the catalyst was done using inductively coupled plasma optical emission spectrometry (ICP-OES) using an OPTIMA 7300DV analyzer.

2.2. Materials and reagents

All reagents and solvents utilized throughout the experiments were obtained from Merck and employed as received without additional purification. The reaction progress and product purity were evaluated *via* thin-layer chromatography (TLC) on silica-gel Polygram SIL G/UV254 plates.

2.2.1 Fabrication of the catalyst

2.2.1.1. Synthesis of Fe-MIL-101-NH_2. Fe-MIL-101-NH_2 was synthesized following a reported method with a slight modification.[52] A solution of 2-amino-1,4-benzenedicarboxylate (0.22 g, 1.24 mmol) in DMF (7.5 mL) was slowly added to a solution of $FeCl_3 \cdot 6H_2O$ (0.67 g, 2.49 mmol) in DMF (7.5 mL). The resulting mixture was heated in a stainless-steel autoclave at 110 °C for 24 h. The solid was isolated by centrifugation, washed with DMF and EtOH (3 × 10 mL), dried at 80 °C under vacuum for 24 h and then dried at ambient temperature.

2.2.1.2. Synthesis of ISA-MIL-Fe. Isatin (0.147 g, 1 mmol) was poured into a mixture containing the as-synthesized Fe-MIL-101-NH_2 (0.13 g) suspended in ethanol (20 mL). The reaction solution was refluxed under stirring for 24 hours. Upon completion, the resulting brown precipitate was collected by centrifugation, rinsed thoroughly with ethanol (3 × 10 mL), followed by vacuum drying at 60 °C to afford ISA-MIL-Fe as a brown solid.

2.2.1.3. Synthesis of Cu-ISA-MIL-Fe. To the well-dispersed ethanolic suspension of ISA-MIL-Fe (0.1 g, in 15 mL ethanol), $Cu(OAc)_2 \cdot 4H_2O$ (0.05 g, 0.2 mmol) was added under continuous stirring. The reaction mixture was then subjected to reflux under continuous stirring for 24 hours, allowing for the effective coordination of copper within the Schiff-base-modified framework. After completion of the reaction, the resulting solid was separated by centrifugation, washed thoroughly with EtOH (3 × 10 mL), and dried in a vacuum oven. Based on ICP-OES analysis, the copper amount in Cu-ISA-MIL-Fe was determined to be 2.28 mmol per gram of the catalyst.

2.3. Catalytic tests

2.3.1. General procedure for the direct one-pot one-step synthesis of dialkyl α-aminophosphonates from alcohols *via* TOP in the presence of Cu-ISA-MIL-Fe. To a mixture of benzyl alcohol (1 mmol), aniline (1 mmol), trialkyl/dialkyl phosphite (1 mmol) and *t*-butyl hydroperoxide (TBHP, 1 mmol) in EtOH (5 mL), Cu-ISA-MIL-Fe (2 mol%, 0.0088 g) was added. The reaction mixture was stirred under reflux conditions upon completion, as monitored by TLC (Table 3). Then, the reaction suspension was diluted with ethanol and subjected to centrifugation to recover the catalyst. The separated catalyst was then washed with ethanol in three portions (5 mL each) and dried overnight at 80 °C for reuse in subsequent cycles. The combined filtrates were concentrated under reduced pressure to afford the crude product, which was finally purified by chromatography on silica

gel using a mixture of *n*-hexane and ethyl acetate (1 : 2) as the eluent.

3. Result and discussion

3.1. Fabrication and characterization of Cu-ISA-MIL-Fe

Cu-ISA-MIL-Fe was fabricated by the route presented in Fig. 1. At first, Fe-MIL-101-NH_2 was synthesized by a solvothermal method from 2-amino-1,4-benzenedicarboxylate and $FeCl_3 \cdot 6H_2O$. Cu-ISA-MIL-Fe was obtained by the PSM of Fe-MIL-101-NH_2, involving Schiff-base formation with isatin, followed by metal coordination using $Cu(OAc)_2$ (Fig. 1).

Fig. 2 represents the PXRD patterns of Fe-MIL-101-NH_2 and Cu-ISA-MIL-Fe. The distinct peaks observed at 2θ of 5.16, 9.0, 9.49, 10.1, and 16.60 (Fig. 2a) are indicative of the well-defined crystalline nature of Fe-MIL-101-NH_2,[53] which is in good agreement with the previously reported diffraction pattern for Fe-MIL-101-NH_2. The similarity of the indexed diffraction peaks of Cu-ISA-MIL-Fe (Fig. 2b) with those of Fe-MIL-101-NH_2 endorses that the MOF structure remained intact during the PSM process.

The FT-IR spectra of Fe-MIL-101-NH_2, ISA-MIL-Fe and Cu-ISA-MIL-Fe (Fig. 3) confirm the successful construction and functionalization of the desired MOF. As shown in Fig. 3a, the spectrum of Fe-MIL-101-NH_2 reveals characteristic peaks at 1382–1426 (C=C) and 1502–1600 cm^{-1} (C=O), ascribed to the 2-aminoterephthalate functions. Additionally, a peak is observed at 1257 cm^{-1}, attributed to the C–N bond in the MOF structure. Upon the modification of Fe-MIL-101-NH_2 with isatin, a new broad peak appeared at 1705 cm^{-1} (C=O), which clearly certified the functionalization of the MOF with isatin groups (Fig. 3b). Moreover, the stretching peak of the C=N group appears to be present at approximately 1630 cm^{-1}, but it is obscured due to the overlap with the strong carbonyl peak. Further modification of ISA-MIL-Fe with copper led to shifts in the vibration frequencies of the C=O and C=N groups of isatin to lower values, with a slight intensity decrease, confirming the successful metal–ligand coordination (Fig. 3c).

As evidenced by FESEM and TEM images (Fig. 4), the octahedral morphology of Cu-ISA-MIL-Fe remains nearly unchanged after the PSM of Fe-MIL-101-NH_2. This

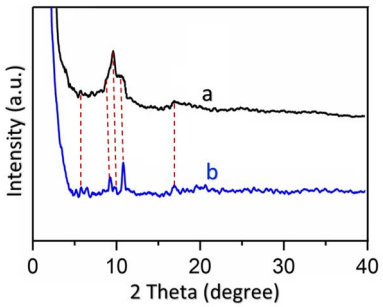

Fig. 2 PXRD patterns of (a) Fe-MIL-101-NH_2 and (b) Cu-ISA-MIL-Fe.

morphological retention upon Cu-functionalization[54] offers a crucial advantage as it ensures that the structural integrity of the MOF remains intact, which is essential for a good catalytic performance. Fig. 4 displays the well-defined regular octahedral structures of Fe-MIL-101-NH_2 and Cu-ISA-MIL-Fe, characterized by 8 facets, 6 vertices, and 12 edges, with sharp corners and smooth surfaces. The octahedral structure of Cu-ISA-MIL-Fe has an edge length of approximately 500 nm (Fig. 4d).

XPS analysis was employed to investigate the surface electronic characteristics of and elemental distribution on the Cu-ISA-MIL-Fe surface (Fig. 5). XPS elemental survey of Cu-ISA-MIL-Fe clearly confirms the existence of carbon, oxygen, nitrogen, copper, and iron elements in this compound (Fig. 5a). In the C 1s spectrum, the carbon peak is divided into four peaks, including 284.7 (C–C), 285.3 (C=N), 286.0 (C–N), and 288.3 eV (C=O) (Fig. 5b).[55] Fig. 5c demonstrates the high-resolution XPS spectrum for N 1s, revealing three prominent peaks at 398.5, 399.7 and 400.0 eV, corresponding to the C=N, C–N and N–H bonds, respectively.[56] The high-resolution XPS profile of O 1s discloses characteristic signals corresponding to the Fe–O–Fe, Fe–O–H, and O–C=O bonding environments, which are consistent with the binding energies of 530.0, 531.6, and 533.4 eV, respectively (Fig. 5d).[57,58] The Fe 2p spectrum presents distinct peaks at 710.1 and 711.3 eV, consistent with Fe $2p_{3/2}$ and at 723.0 and 724.7 eV, attributed to Fe $2p_{1/2}$. Additionally, satellite peaks are observed at 713.1 and 716.8 for Fe $2p_{3/2}$ and at 726.5 and 729.7 eV for Fe $2p_{1/2}$ (Fig. 5e).[59] These observations are consistent with the presence of Fe^{3+} species, indicating that the

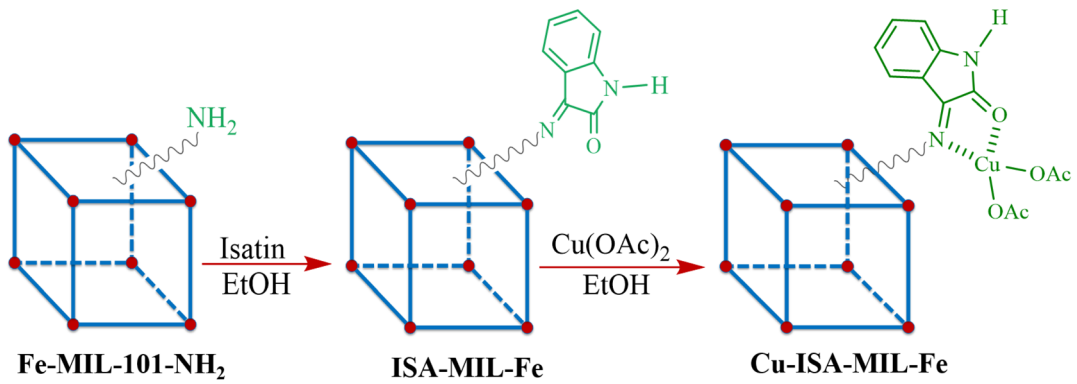

Fig. 1 Schematic of the catalyst preparation steps.

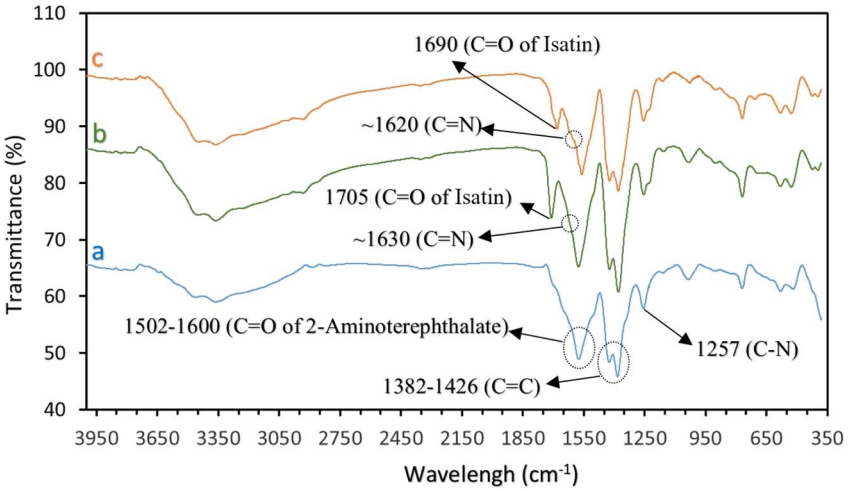

Fig. 3 FT-IR spectra of (a) Fe-MIL-101-NH_2, (b) ISA-MIL-Fe and (c) Cu-ISA-MIL-Fe.

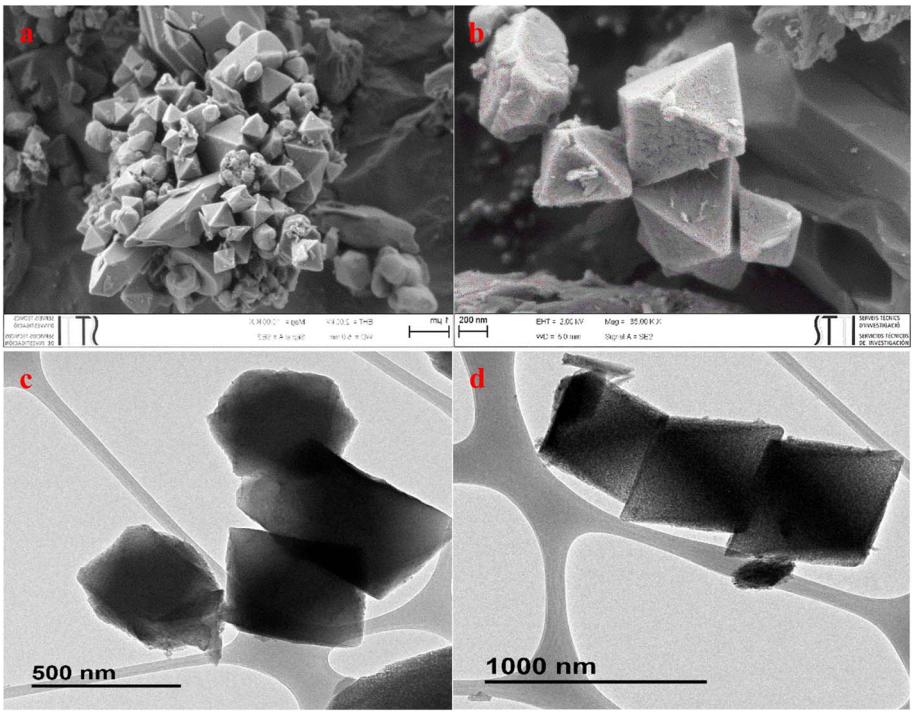

Fig. 4 FESEM images of (a) Fe-MIL-101-NH_2 and (b) Cu-ISA-MIL-Fe. TEM images of (c) Fe-MIL-101-NH_2 and (d) Cu-ISA-MIL-Fe.

iron cations in the catalyst predominantly exist in the +3 oxidation state.[59] In the Cu 2p spectrum, five peaks can be detected at 932.8, 934.5, 937.5, 940.7, and 944.2 eV, corresponding to Cu $2p_{3/2}$, while the fitting peaks at 952.8, 954.2, 956.3, 961.4 and 963.4 eV are associated with Cu $2p_{1/2}$ (Fig. 5f).[60] These findings are consistent with the existence of Cu^{2+} species in the catalyst.[60]

The existence of carbon, nitrogen, oxygen, iron and copper in Cu-ISA-MIL-Fe is confirmed by the EDS spectrum (Fig. 6). Furthermore, EDS elemental mapping displays a homogeneous distribution of these constituents throughout the MOF (Fig. 6).

3.2. Investigation of the catalytic activity of Cu-ISA-MIL-Fe for the one-pot one-step fabrication of dialkyl α-aminophosphonates directly from alcohols *via* TOP

Initially, to evaluate the catalytic activity of Cu-ISA-MIL-Fe for the synthesis of α-aminophosphonates, a model three-component reaction was carried out using benzyl alcohol (1 mmol), aniline (1 mmol) and triethyl phosphite (1 mmol) in the presence of TBHP (1 mmol) as an oxidant. The influence of influential factors comprising the catalyst loading, oxidant, solvent and reaction temperature was monitored to select the optimum reaction conditions for the synthesis of the desired diethyl α-aminophosphonate (Table 1). Based on the obtained

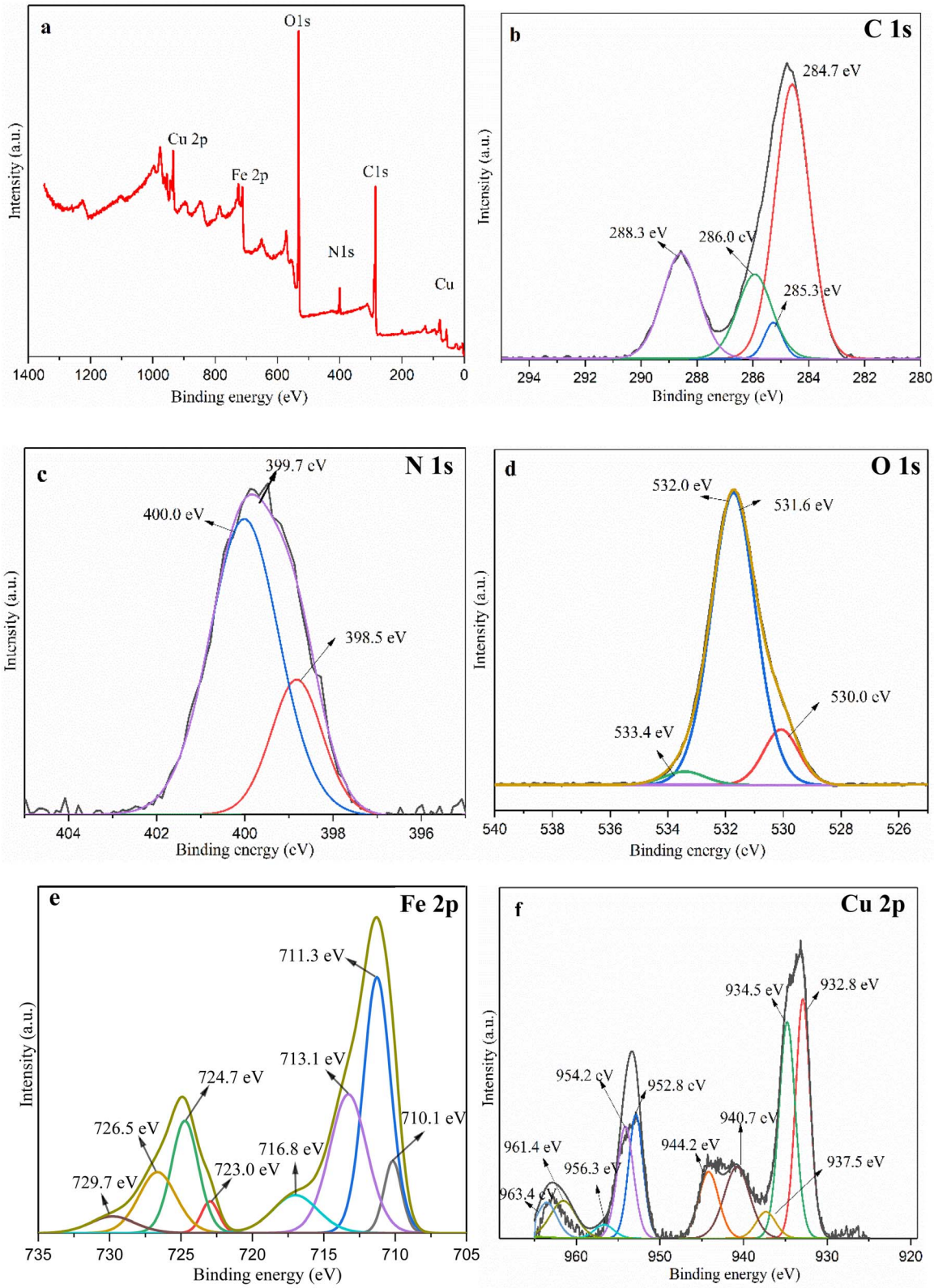

Fig. 5 XPS spectrum of Cu-ISA-MIL-Fe: (a) survey, (b) C 1s, (c) N 1s, (d) O 1s, (e) Fe 2p and (f) Cu 2p.

results, the highest product efficiency was achieved when 2 mol% of Cu-ISA-MIL-Fe was used in ethanol under reflux conditions (Table 1, entry 6). Importantly, a control experiment without the catalyst resulted in no detectable product (Table 1, entry 1). Furthermore, only a negligible yield of the target product was obtained using $Cu(OAc)_2$ as the catalyst, under

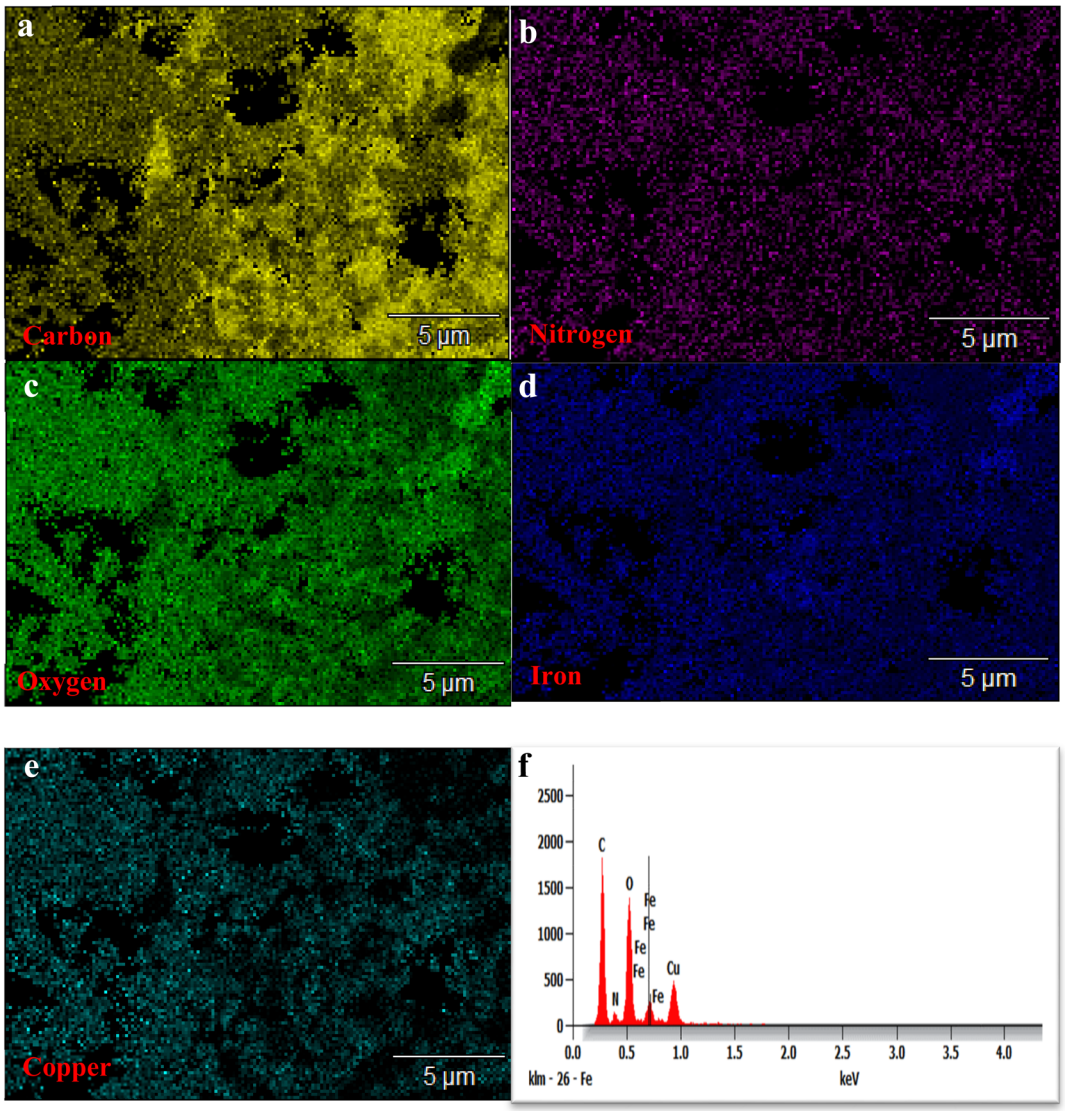

Fig. 6 Elemental mapping images of (a) C, (b) N, (c) O, (d) Fe and (e) Cu, and (f) EDS spectrum of Cu-ISA-MIL-Fe.

similar reaction conditions (Table 1, entry 19). In addition, when the model reaction was carried out in the presence of other kinds of oxidants (Table 1, entries 14–17) and without the oxidant (Table 1, entry 18), the results were far from satisfactory.

In a complementary experiment designed to gain deeper insights into the vital role of Cu-ISA-MIL-Fe in the synthesis of α-aminophosphonates, as well as to compare the reactivity of benzyl alcohol *versus* that of benzaldehyde as a starting substance, the model reaction was further investigated. All of the reactions were performed in ethanol under reflux conditions. The obtained findings are listed in Table 2. Initially, the model reaction was performed using benzaldehyde instead of benzyl alcohol as the precursor in the presence of Cu-ISA-MIL-Fe, without any external oxidant. This reaction afforded the desired product in 95% yield within 1.5 h (Table 2, entry 1). Subsequently, the same reaction was accomplished using Fe-MIL-101-NH_2 as the catalyst. However, the results were unsatisfactory even after 6 h (Table 2, entry 2). To evaluate the catalytic effect on the oxidation of benzyl alcohol in the presence of TBHP as the oxidant, a control reaction was conducted in the absence of triethyl phosphite. Remarkably, the reaction proceeded efficiently, yielding 92% of benzaldehyde within 2 h (Table 2, entry 3). To further highlight the catalytic activity of Cu-ISA-MIL-Fe, the same reaction was done using Fe-MIL-101-NH_2 both in the presence and absence of triethyl phosphite. In both cases, the reaction failed to produce significant yields of benzaldehyde and diethyl α-aminophosphonate (Table 2, entries 4 and 5), confirming the superior performance of Cu-ISA-MIL-Fe.

Under the optimized reaction conditions, a variety of α-aminophosphonates were synthesized using different benzyl alcohols, anilines and phosphite esters (Table 3). As depicted in Table 3, dialkyl α-aminophosphonates containing various alkyl ester groups were efficiently synthesized through the TOP strategy by the reaction of benzyl alcohol and aniline with diverse phosphite esters, including triethyl/tri-*iso*-propyl/di-*iso*-

Table 1 Optimization of the reaction conditions by the evaluation of different parameters

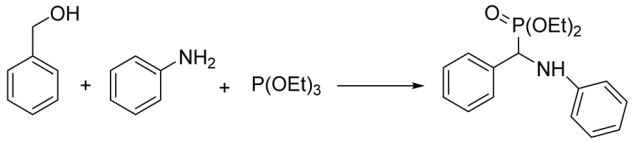

Entry	Catalyst (mol%)[a]	Oxidant	Solvent	Temperature (°C)	Time (h)	Isolated yield (%)[b]
1	—	TBHP	EtOH	Reflux	24	—
2	2	TBHP	H_2O	80	2	43
3	2	TBHP	CH_3CN	Reflux	2	87
4	2	TBHP	DMF	80/130	2	78/80
5	2	TBHP	—	80	24	20
6	2	TBHP	EtOH	Reflux	2	95
7	0.5	TBHP	EtOH	Reflux	2	52
8	1	TBHP	EtOH	Reflux	2	85
9	1.5	TBHP	EtOH	Reflux	2	90
10	2.5	TBHP	EtOH	Reflux	2	95
11	2	TBHP	EtOH	r.t.	6	37
12	2	TBHP	EtOH	50	4	48
13	2	TBHP	EtOH	70	2	85
14	2	H_2O_2 (30%)	EtOH	Reflux	2	36
15	2	O_2	EtOH	Reflux	2	61
16	2	$K_2S_2O_8$	EtOH	Reflux	2	53
17	2	Air	EtOH	Reflux	2	42
18	2	—	EtOH	Reflux	2	32
19	2[c]	TBHP	EtOH	Reflux	2	Trace

[a] According to the copper content (except for entry 1). [b] Reaction conditions: benzyl alcohol (1 mmol), aniline (1 mmol), triethyl phosphite (1 mmol), oxidant (1 mmol) (except for entry 18), solvent (5 mL) (except for entry 5) and Cu-ISA-MIL-Fe (except for entries 1 and 19). [c] Reaction was conducted using the $Cu(OAc)_2$ catalyst.

Table 2 Evaluation of the crucial effect of Cu-ISA-MIL-Fe in the one-pot one-step synthesis of diethyl α-aminophosphonate

Entry	Catalyst	Benzyl alcohol (mmol)	Oxidant	Benzaldehyde (mmol)	Triethyl phosphite (mmol)	Time (h)	Isolated yield[a] (%)
1	Cu-ISA-MIL-Fe	—	—	1	1	1.5	95
2	Fe-MIL-101-NH_2	—	—	1	1	1 (6)	55 (55)
3	Cu-ISA-MIL-Fe	1	TBHP	—	—	1.5	92
4	Fe-MIL-101-NH_2	1	TBHP	—	—	2	35
5	Fe-MIL-101-NH_2	1	TBHP	—	1	2	25

[a] Reaction conditions: benzyl alcohol/benzaldehyde (1 mmol), aniline (1 mmol), triethyl phosphite (1 mmol, except in entries 3 and 4), TBHP (1 mmol, except in entries 1 and 2), catalyst (0.0088 g), EtOH (5 mL), reflux conditions.

propyl and trimethyl phosphites (Table 3, entries 1–4). The reaction of benzyl alcohol with 4-chloroaniline and *p*-toluidine, representing electron-withdrawing and electron-donating derivatives of aniline, respectively, proceeded well with triethyl phosphite, affording the corresponding diethyl α-aminophosphonates in good to high product yields (Table 3, entries 5 and 6). Moreover, benzyl alcohols substituted with either electron-withdrawing or electron-donating groups were well-tolerated under the optimized reaction conditions (Table 3, entries 7–10).

High reusability of catalysts is an important advantage in catalytic methods, enhancing their potential for commercial applications. Thus, the recyclability of Cu-ISA-MIL-Fe was checked in the model reaction. Upon completion of the reaction, the catalyst was recovered by centrifugation, thoroughly washed with EtOH, and subsequently dried overnight. The separated catalyst was reused for five consecutive cycles, with only a slight decrease in the catalytic efficiency observed (Fig. 7a). FESEM images of the reused catalyst after five runs verified that the catalyst retained its original morphological properties throughout the reaction process (Fig. 7b and c).

To realize the true heterogeneity nature of the catalyst, hot filtration and poisoning tests were conducted separately (Fig. 8).

For both, the model reaction was monitored under optimum conditions. In the hot filtration experiment, the catalyst was isolated by filtration once approximately 50% of the reaction was completed, and the reaction mixture was subsequently allowed to continue for an additional 3 hours. The absence of further conversion in the reaction medium confirmed that no homogeneous catalyst was present in the reaction medium. ICP-OES

Table 3 One-pot one-step synthesis of dialkyl α-aminophosphonates directly from alcohols *via* TOP, catalyzed by Cu-ISA-MIL-Fe

Entry	Benzyl alcohol	Amine	Phosphite ester	Product	M.P. (°C) Found	M.P. (°C) Reported[Ref.]	Time (h)	Isolated yield[a] (%)
1	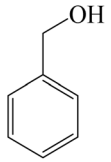	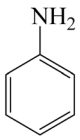	$P(OEt)_3$	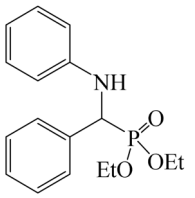	88	86.9 (ref. 61)	2	95
2	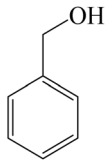	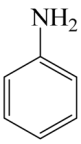	$P(O–iso\text{-}Pr)_3$	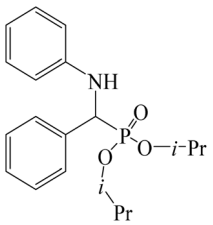	102–104	103–105 (ref. 62)	2	87
3	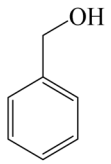	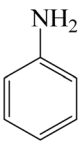	$HP(O)(O\text{-}iso\text{-}Pr)_2$	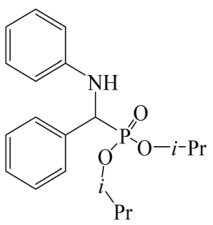	102–104	103–105 (ref. 62)	2	83
4	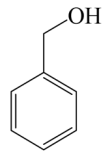	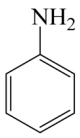	$P(OMe)_3$	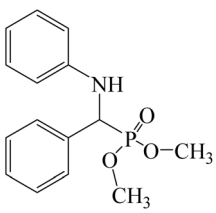	93–94	94–96 (ref. 63)	2	80
5	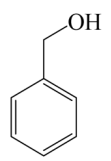	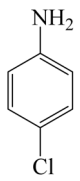	$P(OEt)_3$	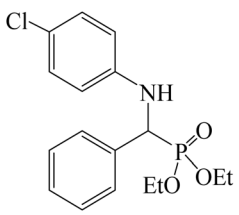	112–113	112–114 (ref. 39)	4	76
6	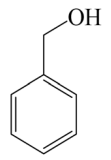	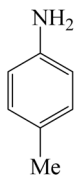	$P(OEt)_3$	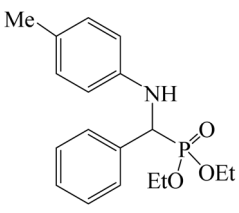	119	120 (ref. 64)	3	86
7	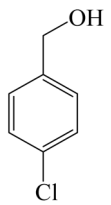	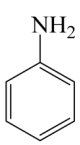	$P(OEt)_3$	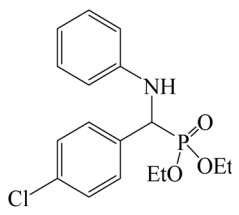	88–87	87.1 (ref. 61)	2	88

Table 3 (*Contd.*)

Entry	Benzyl alcohol	Amine	Phosphite ester	Product	M.P. (°C) Found	M.P. (°C) Reported[Ref.]	Time (h)	Isolated yield[a] (%)
8	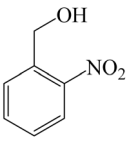	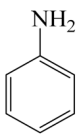	$P(OEt)_3$	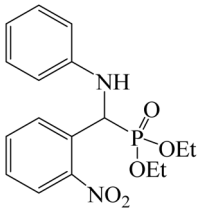	156–155	155–157 (ref. 65)	2	83
9	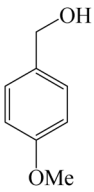	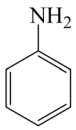	$P(OEt)_3$	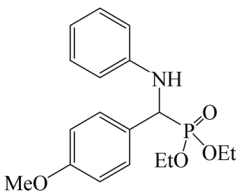	103–104	103 (ref. 64)	2	79
10	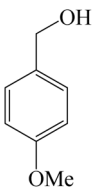	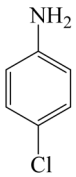	$P(OEt)_3$	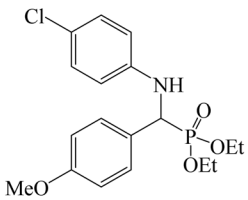	101–102	101–102 (ref. 66)	2	75

[a] Reaction conditions: benzyl alcohol (1 mmol), aniline (1 mmol), phosphite ester (1 mmol), TBHP (1 mmol), catalyst (2 mol%) and EtOH (5 mL) under reflux conditions.

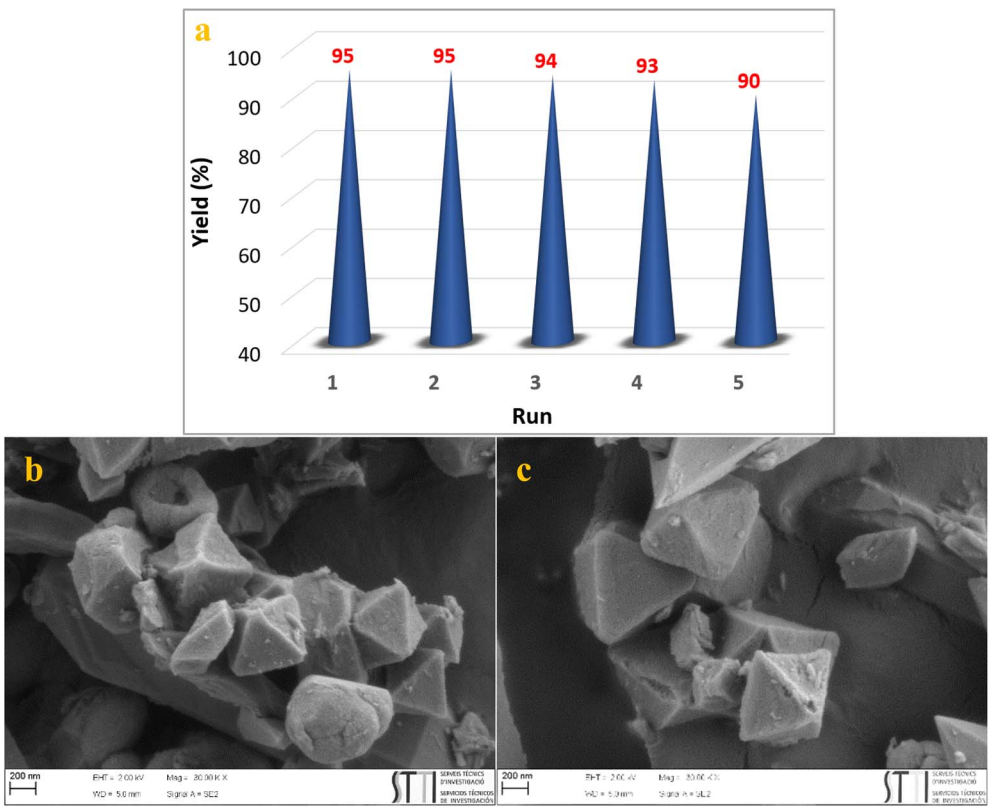

Fig. 7 (a) Reusability of Cu-ISA-MIL-Fe in the model reaction. (b and c) FESEM images of the recovered Cu-ISA-MIL-Fe after five runs.

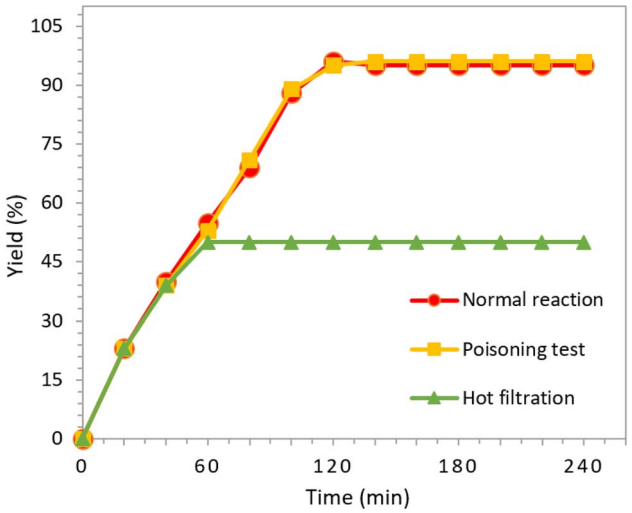

Fig. 8 Study of the heterogeneity of the catalyst.

analysis of the filtrate revealed a negligible Cu content (less than 0.1% of the total Cu amount). In the poisoning test, the model reaction was done in the presence of elemental sulfur (S_8, 0.07 g) as a metal scavenger. Under this condition, the reaction progressed normally with no change in rate. These results clearly affirmed the true heterogeneous function of the catalyst.

In the next step, the advantages of the current catalytic pathway were compared with those of the previously reported systems that enable the direct transformation of alcohols into α-aminophosphonates (Table 4). The results clearly demonstrate that the present tandem approach enables a milder, more straightforward, and eco-friendly transformation, proceeding efficiently in the presence of a recyclable heterogeneous catalyst *via* a one-pot one-step procedure. In contrast, all methods reported to date, except one, proceed through a one-pot two-step pathway, which requires two distinct reaction steps.[35–38] In the only one-pot one-step method, Pd, an expensive catalyst, was used.[39] Furthermore, all of these routes suffer from one or more limitations, including the use of hazardous solvents;[35,36,38,39] strict reaction conditions;[35–39] extended reaction times;[35,36,38] low product yields;[36,38] non-recyclable homogeneous catalytic systems;[35,38] and structurally complex,[35] expensive,[39] or even explosive catalysts.[37] These comparisons highlight the practical superiority and synthetic simplicity of the present methodology over previously reported protocols.

By analogy with our investigation and based on a survey of the literature,[67–73] a plausible mechanistic pathway for the direct fabrication of dialkyl α-aminophosphonates from alcohols *via* TOP in the presence of Cu-ISA-MIL-Fe is outlined in Scheme 3. In the first step, TBHP is converted into *tert*-butoxyl (*t*-BuO$^{\cdot}$) and hydroxyl (HO$^{\cdot}$) radicals mainly by the Cu and less by the Fe present in Cu-ISA-MIL-Fe. Then, *t*-BuO$^{\cdot}$ abstracts a hydrogen atom from benzyl alcohol, forming a benzyl radical intermediate (I). The activated intermediate (I) with the catalyst undergoes further oxidation by HO$^{\cdot}$ to generate benzaldehyde as the final oxidation product. Subsequently, mainly the copper and/or less the iron in the catalyst act as Lewis acids to activate the carbonyl group of benzaldehyde, facilitating a nucleophilic attack by aniline, which leads to the formation of the corresponding imine (II) with the release of water. Then, the activated carbon center in the imine by copper and/or less by iron undergoes nucleophilic addition with phosphite ester. This transformation ultimately yields the desired dialkyl α-aminophosphonate, after which the catalyst regenerates and re-enters the catalytic cycle (Scheme 3). During the condensation reaction, the unmodified amine groups in Cu-ISA-MIL-Fe can act as Brønsted basic sites to abstract hydrogen. Based on the results in Table 2, the most active site of the catalyst is copper in Cu-ISA-MIL-Fe.

Table 4 Comparison of the reaction conditions for Cu-ISA-MIL-Fe with those for other reported catalysts for the synthesis of diethyl (phenyl)-*N*-(phenyl)aminomethylphosphonate directly from alcohols

Entry[Ref.]	Catalyst (amount)	Reaction conditions	Time (h)	Yield (%)
1 (ref. 35)	First step: Iron-based Knolker's complex (6.3 mol%); Second step: Chiral phosphoric acids (8.3 mol%)	First step: *p*-xylene, MS[a] (3 Å), 140 °C, 55 h second step: 25 °C, 24 h	79	81
2 (ref. 36)	CuO@Fe_3O_4 (1.5 mol%)	First step: toluene, NaOH (1.5 equiv.), 100 °C, 4 days; second step: 100 °C, 24 h	120 (5 days)	70
3 (ref. 37)	NH_4ClO_4 (100 mol%)	First step: UV irradiation, O_2, solvent-free second step: 50 °C	4	93
4 (ref. 38)	TBATB[b] (1 mol%)	First step: CH_3CN, blue LED (465 nm, 4*3 W); 3 h, air second step: Reflux, 5 h, EtOAc : CH_3CN (5 : 3)	8	75
5 (ref. 39)	Pd-HAP[c] (0.2 mol% Pd)	°C 90 toluene, O_2	6	87
6[this work]	Cu-ISA-MIL-Fe (2 mol%)	TBHP, EtOH, reflux	2	95

[a] MS: molecular sieves. [b] TBATB: tetrabutylammonium tribromide. [c] HAP: hydroxyapatite.

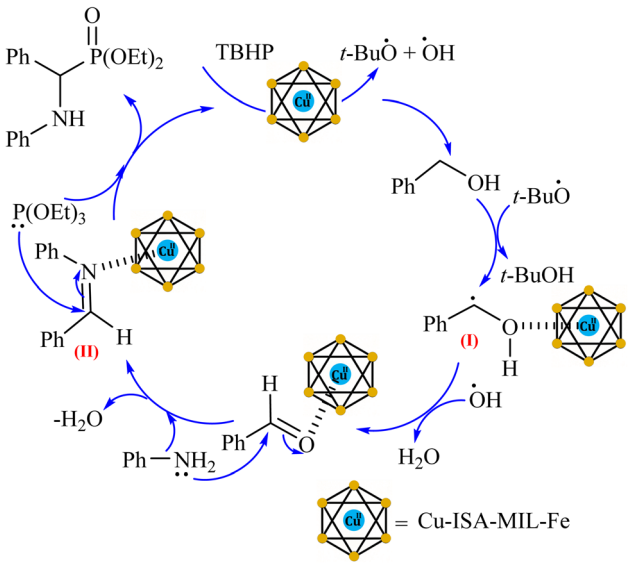

Scheme 3 Plausible mechanism for the direct synthesis of dialkyl α-aminophosphonates from alcohols.

4. Conclusions

In this study, Cu-ISA-MIL-Fe was synthesized by the PSM of Fe-MIL-101-NH_2 through Schiff-base formation with isatin, followed by a reaction with $Cu(OAc)_2$. After the characterization of this new catalyst with different methods, it was used as the first MOF-based heterogeneous catalyst for the successful one-pot one-step fabrication of dialkyl α-aminophosphonates directly from alcohols *via* TOP. The catalyst showed an extremely high catalytic performance for the oxidation of different benzyl alcohols, followed by the condensation of the *in situ* prepared benzaldehyde with anilines and various alkyl phosphites to produce a variety of dialkyl α-aminophosphonates. This approach offers several advantages, such as good to high yields of the products, short reaction times, the use of a simplified one-pot one-step synthetic process with step saving and the least amount of waste production, use of green solvents, low operational cost and facile catalyst recovery and reuse. Besides, the hot filtration test and poisoning experiment affirmed that the catalytic reaction followed a real heterogeneous pathway. Considering its remarkable catalytic efficiency, operational simplicity and sustainability, Cu-ISA-MIL-Fe holds great promise for future applications in diverse green synthetic methodologies.

Author contributions

S. Sobhani served as the research supervisor and corresponding author. A. R. Pasban conducted all the synthesis works. S. Sobhani and R. Jahanshahi wrote the manuscript. J. M. Sansano carried out TEM and XPS analyses.

Conflicts of interest

There are no conflicts to declare.

Data availability

The data supporting this article have been included as part of the SI. Supplementary information is available. See DOI: https://doi.org/10.1039/d5ra06341h.

Acknowledgements

We thank the University of Birjand Research Council for supporting this work and the University of Alicante for access to the TEM and XPS analyses. All assistance from M. Rouzifar to A. R. Paseban for conducting MOF synthesis and analysis is acknowledged.

References

1 P. T. Anastas and J. C. Warner, *Green Chemistry: Theory and Practice*, Oxford University Press, Oxford, 2000.
2 P. Wender, *Chem. Ind.*, 1997, **19**, 765.
3 L. F. Tietze, *Chem. Rev.*, 1996, **96**, 115–136.
4 K. C. Nicolaou, D. J. Edmonds and P. G. Bulger, *Angew. Chem., Int. Ed.*, 2006, **45**, 7134–7186.
5 O. Kayser and N. J. H. Averesch, in *Technical Biochemistry*, Springer Fachmedien Wiesbaden, 2025, ch. 4, DOI: 10.1007/978-3-658-47121-7-4.
6 J. Clayden, N. Greeves and S. Warren, *Organic Chemistry*, Oxford University Press, Oxford, 2nd edn, 2012, ch. 3, pp. 215–240.
7 C. Xu, C. Zhang, H. Li, X. Zhao, L. Song and X. Li, *Catal. Surv. Asia*, 2016, **20**, 13–22.
8 V. Jeena and R. S. Robinson, *RSC Adv.*, 2014, **4**, 40720–40739.
9 B. Kaboudin, P. Daliri, S. Faghih and H. Esfandiari, *Front. Chem.*, 2022, **10**, 890696–890712.
10 M. Ordóñez and C. Cativiela, *Tetrahedron*, 2007, **63**, 8933–8958.
11 C. S. Demmer, N. Krogsgaard-Larsen and L. Bunch, *Chem. Rev.*, 2011, **111**, 7981–8006.
12 S. Bhagat and M. Sharma, *Curr. Org. Chem.*, 2012, **16**, 2355–2372.
13 B. Kaboudin, K. Moradi and T. Yokomatsu, *Arkivoc*, 2015, **ii**, 121–146.
14 Q. Han, Y. Wang, Y. Liu, Y. Zhang, Y. Li and Y. Zhao, *Phosphorus Sulfur Silicon Relat. Elem.*, 2020, **195**, 1149–1161.
15 G. Keglevich and P. Keglevich, *Phosphorus Chem. Rev.*, 2019, **5**, 101–120.
16 R. Murugan, S. Balu, S. Arya, R. Atchudan, P. Sivaperumal and T. S. Kannan, *Ind. Eng. Chem. Res.*, 2021, **60**, 4567–4582.
17 L. Zhang and J. Wang, *J. Agric. Food Chem.*, 2018, **66**, 3753–3762.
18 V. P. Kukhar and H. R. Hudson, *Aminophosphonic and Aminophosphinic Acids: Chemistry and Biological Activity*, Wiley, Chichester, 2000.
19 G. V. Shitre and M. B. Suwarnkar, *Int. J. Sci. Res. Sci. Technol.*, 2024, **11**, 21.
20 B. Song, L. Jin, S. Yang and P. S. Bhadury, in *Environment-Friendly Antiviral Agents for Plants*, Springer, 2010, ch. 2, pp. 7–93.

21 I. E. T. El Sayed, G. Fathy and A. A. S. Ahmed, *Biomed. J. Sci. Tech. Res.*, 2019, **23**, 17609–17614.
22 G. Keglevich and E. Bálint, *Molecules*, 2012, **17**, 12821–12835.
23 P. R. Varga and G. Keglevich, *Molecules*, 2021, **26**, 2511–2538.
24 A. Amira, Z. Aouf, H. K'tir, Y. Chemam, R. Ghodbane, R. Zerrouki and N. E. Aouf, *ChemistrySelect*, 2021, **6**, 6137–6149.
25 T. M. Shaikh and M. R. Munavalli, *Tetrahedron Lett.*, 2019, **60**, 150–160.
26 V. Gupta and S. Gupta, *Catalysts*, 2020, **10**, 770–790.
27 S. S. Ghodke, P. M. Khandare, R. D. Ingle and R. P. Pawar, *Lett. Appl. NanoBioSci.*, 2022, **11**, 3175–3180.
28 S. Ahmed, M. A. Khan, A. Kumar, R. Singh, P. Sharma and N. Verma, *J. Mol. Catal. A: Chem.*, 2022, **424**, 115253–115264.
29 M. Ferrah, S. Guezane-Lakoud, H. Bendjeffal, R. Aissa, M. Merabet-Khelassi, M. Toffano and L. Aribi-Zouioueche, *React. Kinet. Mech. Catal.*, 2023, **136**, 165–182.
30 B. C. Ranu and A. Hajra, *Green Chem.*, 2002, **4**, 551–554.
31 S. R. Mandha, M. Alla and V. R. Bommena, *J. Chem. Sci.*, 2014, **126**, 793–799.
32 G. Sravya, A. Balakrishna, G. V. Zyryanov, G. Mohan, C. Suresh Reddy and N. B. Reddy, *Phosphorus Sulfur Silicon Relat. Elem.*, 2021, **196**, 353–381.
33 E. Bálint, A. Tripolszky, Á. Tajti and G. Keglevich, in *Organophosphorus Chemistry: Novel Developments*, ed. G. Keglevich, De Gruyter, Berlin, 2018, ch. 6, DOI: **10.1515/9783110535839-006**.
34 M. K. Kolli, P. Elamathi, G. Chandrasekar, V. R. Katta and G. B. Raolji, *Synth. Commun.*, 2018, **48**, 638–649.
35 N. Hofmann and K. C. Hultzsch, *Eur. J. Org Chem.*, 2019, **2019**, 3105–3111.
36 B. Kaboudin, F. Kazemi and N. K. Hosseini, *Res. Chem. Intermed.*, 2017, **43**, 4475–4486.
37 G. Ali, N. A. Dangroo, S. Raheem, T. Naqvi, T. Ara and M. A. Rizvi, *Acta Chim. Slov.*, 2020, **67**, 195–202.
38 F. Kazemi, Y. Shariati and B. Kaboudin, *ChemistrySelect*, 2022, **7**, e202104220.
39 S. R. Kale, V. G. Kalalawe, J. M. Kondre, S. S. Kahandal and S. T. Disale, *Bull. Chem. Soc. Jpn.*, 2024, **97**, uoae052.
40 A. F. Sahayaraj, H. J. Prabu, J. Maniraj, M. Kannan, M. Bharathi, P. Diwahar and J. Salamon, *J. Inorg. Organomet. Polym. Mater.*, 2023, **33**, 1757–1781.
41 T. Gadzikwa and P. Matseketsa, *Dalton Trans.*, 2024, **53**, 1234–1250.
42 W. He, Y. Liu, J. Zhang, X. Chen, H. Wang, Q. Li and Z. Zhao, *J. Mater. Chem. A*, 2023, **11**, 14567–14589.
43 A. Biswas, in *Sustainable Chemical Insight in Biological Exploration*, ed. H. S. Biswas, A. Ghosh, S. Poddar, S. A. I. S. M. Ghazali and A. Bhaumik, Lincoln University College, Petaling Jaya, Malaysia, 2024.
44 Y. Song and S. Ma, *Chem. Sci.*, 2025, **16**, 11740–11767.
45 Z. Ji, H. Wang, S. Canossa, S. Wuttke and O. M. Yaghi, *Adv. Funct. Mater.*, 2020, **30**, 2000238–2000249.
46 D. Lee, S. Lee, I. Choi and M. Kim, *Smart Mol.*, 2024, **2**, e20240002.
47 N. Ko, J. Park, M. P. Suh, Y. Jung, J. K. Kang, S. H. Jhung and A. Coskun, *J. Mater. Chem. A*, 2015, **3**, 2057–2062.
48 (*a*) A. Vigroux, C. Lherbet, I. Fabing, M. C. Barthélémy, C. Laurent and P. Hoffmann, *Chemistry*, 2025, **7**, 48; (*b*) Y. Lin, C. Kong and L. Chen, *RSC Adv.*, 2016, **6**, 32598–32614; (*c*) N. Sunder, Y. Y. Fong, M. A. Bustam and N. H. Suhaimi, *Polymers*, 2022, **14**, 1408–1434; (*d*) T. Gadzikwa and P. Matseketsa, *Dalton Trans.*, 2024, **53**, 7659–7668; (*e*) V. D. Manvatkar and R. S. Dongre, *Chem. Afr.*, 2025, **8**, 419–435.
49 H. Kim, Y. Son, D. Hwang, P. C. Rao, Y. Kim and M. Yoon, *Chem Asian J.*, 2025, e202401614.
50 (*a*) Z. Wang, X. Luo, B. Zheng, L. Huang, C. Hang, Y. Jiao, X. Cao, W. Zeng and R. Yun, *Eur. J. Inorg. Chem.*, 2018, 1309–1314; (*b*) Z. Miaoa, Y. Luanb, C. Qib and D. Ramella, *Dalton Trans.*, 2016, **45**, 13917–13924; (*c*) Z. Shi, G. Niu, Q. Han, X. Shi and M. Li, *Mol. Catal.*, 2018, **461**, 10–18.
51 (*a*) S. Sobhani, H. H. Moghadam, S. R. Derakhshan and J. M. Sansano, *RSC Adv.*, 2021, **11**, 19121–19127; (*b*) M. Rouzifar, S. Sobhani, A. Farrokhi and J. M. Sansano, *Sci. Rep.*, 2023, **13**, 5115–135128; (*c*) F. Omarzehi Chahkamali, S. Sobhani and J. M. Sansano, *Sci. Rep.*, 2022, **12**, 2867–122887; (*d*) M. Rouzifar, S. Sobhani, A. R. Farokhi and J. M. Sansano, *J. Photochem. Photobiol. A: Chem.*, 2024, **447**, 115263–115274.
52 D. Wang and Z. Li, *Catal. Sci. Technol.*, 2015, **5**, 1623–1628.
53 R. Liu, L. Chi, X. Wang, Y. Wang, Y. Sui, T. Xie and H. Arandiyan, *Chem. Eng. J.*, 2019, **357**, 159–168.
54 (*a*) T. Toyao, K. Miyahara, M. Fujiwaki, T.-H. Kim, S. Dohshi, Y. Horiuchi and M. Matsuoka, *J. Phys. Chem. C*, 2015, **119**, 8131–8137; (*b*) L. Xiao, Q. Zhang, P. Chen, L. Chen, F. Ding, J. Tang, Y.-J. Li, Ch.-T. Au and S.-F. Yin, *Appl. Catal. B*, 2019, **248**, 380–387; (*c*) J. Hou, Y. Luan, J. Tang, A. M. Wensley, M. Yang and Y. Lu, *J. Mol. Catal. A: Chem.*, 2015, **407**, 53–59.
55 Z. Zhang, X. Li, B. Liu, Q. Zhao and G. Chen, *RSC Adv.*, 2016, **6**, 4289–4295.
56 J. Wang, M. Yang, W. Dong, Z. Jin, J. Tang, S. Fan, Y. Lu and G. Wang, *Catal. Sci. Technol.*, 2016, **6**, 161–168.
57 A. Zhang, J. Wu, L. Xue, S. Yan and S. Zeng, *Inorg. Chem.*, 2020, **59**, 403–414.
58 S. Ravichandran, N. Bhuvanendran, K. Peng, W. Zhang, Q. Xu and H. Su, *J. Electrochem. Energy Convers. Storage*, 2021, **18**, 021006–021015.
59 M. C. Biesinger, B. P. Payne, A. P. Grosvenor, L. W. M. Lau, A. R. Gerson and R. S. C. Smart, *Appl. Surf. Sci.*, 2011, **257**, 2717–2730.
60 M. C. Biesinger, *Surf. Interface Anal.*, 2017, **49**, 1325–1334.
61 A. Y. Benzaim, Z. Cheraiet, S. Guezane-Lakoud, A. Zadem and A. Boukhari, *J. Indian Chem. Soc.*, 2025, **102**, 101593–101604.
62 B. Kaboudin, S. Faghih, S. Alavi, M. R. Naimi-Jamal and A. Fattahi, *Synthesis*, 2023, **55**, 121–130.
63 M. S. Haghayegh, N. Azizi, S. S. Shahabi and Y. Gu, *J. Mol. Liq.*, 2023, **387**, 122677–122690.
64 S. Guezane-Lakoud, M. Ferrah, M. Merabet-Khelassi, N. Touil, M. Toffano and L. Aribi-Zouioueche, *J. Biomol. Struct. Dyn.*, 2024, **42**, 3332–3348.

65 T. Piri, R. Peymanfar, S. Javanshir and S. Amirnejat, *Catal. Lett.*, 2019, **149**, 3384–3394.
66 Y. Q. Yu, *Synthesis*, 2013, **45**, 2545–2550.
67 M. Sarkheil and M. Lashanizadegan, *Appl. Organomet. Chem.*, 2017, **31**, e3726.
68 Ç. Akkol, S. Karaböcek, E. T. Saka and B. S. Cevrimli, *Turk. J. Anal. Chem.*, 2024, **6**, 129–137.
69 U. Junghans, C. Suttkus, J. Lincke, D. Lässig, H. Krautscheid and R. Gläser, *Microporous Mesoporous Mater.*, 2015, **216**, 151–160.
70 A. Farrokhi, M. Jafarpour and R. Najafzade, *Catal. Lett.*, 2017, **147**, 1714–1721.
71 L. M. Frija, *J. Chem. Sci.*, 2025, **137**, 1–10.
72 J. Kodchasee, C. Chanloi, P. Khemthong, B. Uapipatanakul, M. Ehara and K. Bobuatong, *Catalysts*, 2021, **11**, 720–733.
73 Y. S. Duh, H. Y. Kuo and C. S. Kao, *J. Therm. Anal. Calorim.*, 2017, **127**, 1047–1059.